[31] Sumida Y, Nakashima T, Yoh T, Nakajima Y, Ishikawa H, Mitsuyoshi H, et al. Serum thioredoxin levels as an indicator of oxidative stress in patients with hepatitis C virus infection. J Hepatol 2000;33(4): 616-622.

[32] Bruix J. Treatment of hepatocellular carcinoma. Hepatology 1997;25(2): 259-262.

[33] Szklaruk J, Silverman PM, Charnsangavej C. Imaging in the diagnosis, staging, treatment, and surveillance of hepatocellular carcinoma. Am J Roentgenol 2003;180(2): 441-454.

[34] Kudo M, Takamine Y, Nakamura K, Shirane H, Uchida H, Kasakura S, et al. Des-gamma-carboxy prothrombin (PIVKA-II) and alpha-fetoprotein-producing IIc-type early gastric cancer. Am J Gastroenterol 1992;87(12): 1859-1862.

[35] Takano S, Honda I, Watanabe S, Soda H, Nagata M, Hoshino I, et al. PIVKA-II-producing advanced gastric cancer. Int J Clin Oncol 2004;9(4): 330-333.

Table 1. Summary of patient information

Clinical information		Training cohort (n=162)	Defect no.	Validation cohort (n=75)	Defect no.	p-value
Age (yr)	Median	61	0	66	0	0.47
	Interquartile range	51 – 73	0	55 – 70	0	
Sex (no.)	Male	73	0	52	0	0.0007*
	Female	89	0	23	0	
AST (UL^{-1})	C	21.5 ± 5.40	0	25.3 ± 3.60	0	0.074
	DI	274 ± 567	0	81.2 ± 84.9	0	0.15
	AHB	25.0 ± 6.81	2	23.9 ± 6.90	0	0.71
	CHB	109 ± 164	0	150 ± 146	0	0.0059
	CNALT	24.1 ± 3.80	0	23.8 ± 6.00	0	0.72
	CHC	62.8 ± 65.3	0	110 ± 51.0	0	0.0010
	CIR	54.6 ± 27.1	0	58.0 ± 26.1	0	0.69
	HCC	71.3 ± 52.8	0	35.0 ± 24.5	0	0.0010
	SS	41.2 ± 11.5	0			
	NASH	78.6 ± 48.0	0			
ALT (UL^{-1})	C	17.7 ± 4.70	0	25.0 ± 8.30	0	0.062
	DI	253 ± 343	0	115 ± 132	0	0.15

	AHB	26.6 ± 18.6	2	23.1 ± 5.60	0	0.40
	CHB	117 ± 162	0	173 ± 131	0	0.0060
	CNALT	17.9 ± 4.10	0	21.5 ± 3.60	0	0.074
	CHC	79.4 ± 81.0	0	160 ± 116	0	0.0036
	CIR	40.7 ± 21.9	0	57.3 ± 42.4	0	0.69
	HCC	57.9 ± 58.8	0	25.0 ± 21.6	0	0.0026
	SS	72.2 ± 24.5	0			
	NASH	121 ± 140	0			
γ-GTP	C	20.7 ± 8.60	0	–	4	–
	DI	190 ± 236	0	46.2 ± 29.5	5	0.010
	AHB	31.1 ± 24.1	2	–	7	–
	CHB	52.8 ± 38.1	1	–	7	–
	CNALT	150 ± 5.70	0	–	8	–
	CHC	48.5 ± 36.4	0	–	11	–
	CIR	28.8 ± 17.9	0	49.6 ± 53.1	0	0.17
	HCC	51.2 ± 31.1	0	–	13	–
	SS	61.8 ± 43.7	0			
	NASH	98.7 ± 99.1	0			
AFP	CHC	6.40 ± 7.40	3	–	11	–
	CIR	35.1 ± 71.8	0	14 ± 15.6	0	0.63
	HCC	9.79×10^2	0	7.04×10^3	0	0.024

		$\pm 1.73 \times 10^3$		$\pm 2.52 \times 10^4$		
PIVKA-II	HCC	1.57×10^2	0	7.78×10^3	0	0.022
		$\pm 1.87 \times 10^2$		$\pm 2.77 \times 10^4$		

* Chi-square test. The others *p* values were obtained by the Mann-Whitney U-test.

Table 2. Biomarkers for discriminating each liver disease selected by MLR models.

Group	Biomarker	Coefficient	95% CI		Odds ratio	95% CI		*p*-value
C	(Intercept)	5.77	3.84	8.32	–	–	–	<0.0001
	γ-Glu-Phe	-58.2	-84.3	-39.0	5.16×10^{-26}	2.47×10^{-37}	1.15×10^{-17}	<0.0001
DI	(Intercept)	-3.08	-4.49	-1.94	–	–	–	<0.0001
	ALT	0.020	7.89×10^{-3}	0.034	1.02	1.01	1.03	2.00×10^{-3}
	γ-Glu-Citrulline	-1.55	-5.01	1.13	0.21	6.68×10^{-3}	3.11	0.31
AHB	(Intercept)	-1.52	-3.35	0.63	–	–	–	0.12
	AST	-0.057	-0.15	-4.96×10^{-3}	0.94	0.86	1.00	0.12
	Methionine sulfoxide	0.072	0.018	0.15	1.08	1.02	1.17	0.047
CHB	(Intercept)	-4.52	-6.33	-3.24	–	–	–	<0.0001
	γ-Glu-Thr	1.52	0.65	2.63	4.58	1.91	13.9	2.30×10^{-3}
CNALT	(Intercept)	-0.76	-3.15	1.94	–	–	–	0.55
	ALT	-0.16	-0.34	-0.049	0.85	0.71	0.95	0.032

	γ-Glu-Taurine	0.80	0.43	1.31	2.23	1.54	3.72	3.00×10^{-4}
CHC	(Intercept)	-4.73	-6.39	-3.47	–	–	–	<0.0001
	γ-Glu-Lys	1.27	0.85	1.82	3.57	2.34	6.14	<0.0001
CIR	(Intercept)	-2.79	-4.05	-1.55	–	–	–	<0.0001
	γ-Glu-Ala	1.80	0.42	3.52	6.05	1.52	33.7	0.020
	γ-Glu-Leu	-0.066	-3.06	2.24	0.94	0.047	9.42	0.96
	γ-Glu-Ser	-1.35	-5.35	1.86	0.26	4.77×10^{-3}	6.44	0.41
	γ-Glu-Taurine	-2.28	-5.07	-0.33	0.10	6.27×10^{-3}	0.72	0.064
HCC	(Intercept)	-1.87	-2.90	-0.90	–	–	–	2.00×10^{-4}
	γ-Glu-Ala	-1.13	-2.44	-0.14	0.32	0.087	0.87	0.050
	γ-Glu-Citrulline	3.51	0.45	7.00	33.4	1.57	1.10×10^{3}	0.033
	γ-Glu-Thr	-1.65	-5.12	0.49	0.19	5.95×10^{-3}	1.63	0.27
	γ-Glu-Phe	6.99	-0.52	14.7	1.09×10^{3}	5.92×10^{-1}	2.50×10^{6}	0.063

Note: The en-dashes in the 95% CI columns indicate that these values could not be calculated.

Biomarker and coefficients are used in MLR model to calculating the probability of each disease.

Intercept indicates the constant term in MLR models.

Figure Legends

Figure 1. Heat map representing the hierarchical clustering of 67 compounds in serum samples from controls and patients with various types of liver disease in both cohorts. Each row shows data for a specific metabolite or transaminase, and each column shows data for the healthy controls and patients with liver diseases. The compound concentration in each individual was divided by the average concentration in the healthy controls and the obtained values were then averaged again for each disease. The metabolites highlighted in yellow showed large fold changes (disease/control ratios of >2.5) in an average of seven liver diseases. *p<0.05, **p<0.01, ***p<0.0001, significance difference by the Kruskal–Wallis test. The compounds were clustered based on elucidation distances. Red and green denote relatively high and low concentrations, respectively, compared with the average concentration.

Figure 2. Representative whisker box plots of the serum levels of detected transaminases and metabolites in the training cohort. The horizontal lines indicate the upper median, median and lower median, and the whiskers show the maximum and minimum levels. One plot for AST was outside the range (>500 U L^{-1}). *p<0.05, **p<0.01, ***p<0.0001, significance difference by the Kruskal-Wallis test and Dunn's post test for each marker and two groups in each marker, respectively.

Figure 3. ROC curve analyses of the ability of γ-glutamyl peptides alone or in combination with AST, ALT and methionine sulfoxide to discriminate each group from all other liver diseases and healthy controls. The solid and dashed curves represent the ROC curves for the training and validation cohorts, respectively. AUC_t and AUC_v in each panel indicate the AUC values in the training and validation cohorts, respectively. The group label

indicates the discriminated group from all the other groups by an MLR model. The biomarkers in each panel were used in the MLR model for discriminating the group, e.g. ALT and γ-Glu-Taurine were the biomarkers for discriminating CNALT from the other groups. The coefficients and constant term of the MLR model of these biomarkers were summarized in Table 2.

Figure 4. Whisker box plots and ROC curves of AFP and MLR analyses based on γ-Glu-Phe, γ-Glu-Ala and γ-Glu-Thr for discriminating patients with HCC (*n*=32) from patients with CHC (*n*=35) and CIR (*n*=18).

Figure 5. Biosynthetic mechanism of γ-glutamyl peptides in hepatocytes under (A) reducing conditions and (B) oxidative stress. GCS is feedback-inhibited by GSH under reducing conditions and small amounts of γ-glutamyl dipeptides are synthesized. During oxidative stress, GSH is consumed, leading to GCS activation. This could result in biosynthesis of γ-glutamyl dipeptides, which are then effluxed across the hepatocellular membrane. γ-Glutamyl dipeptides and tripeptides are indicated by γ-Glu-X and Glu-X-Gly, respectively (X=amino acid or amine).

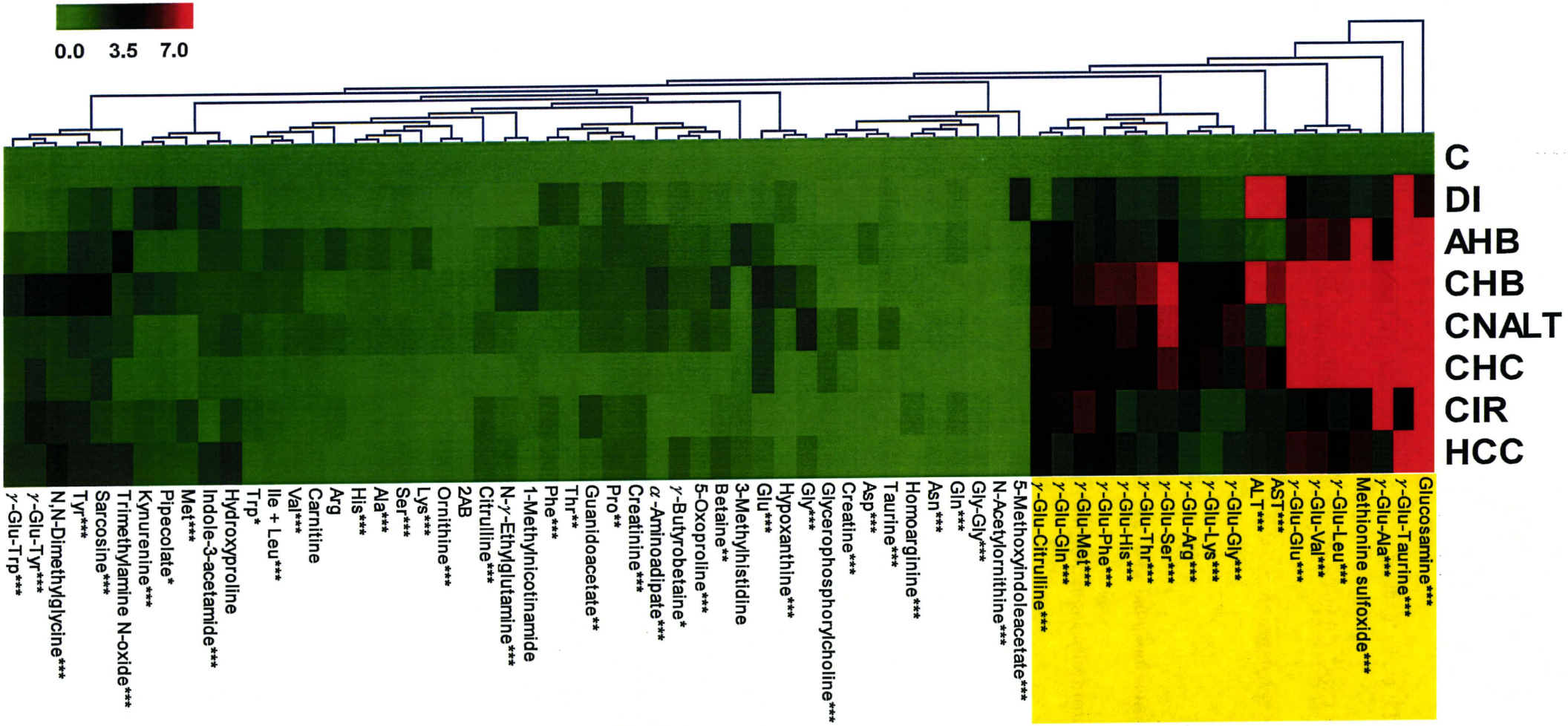

Figure 1 Soga et al.

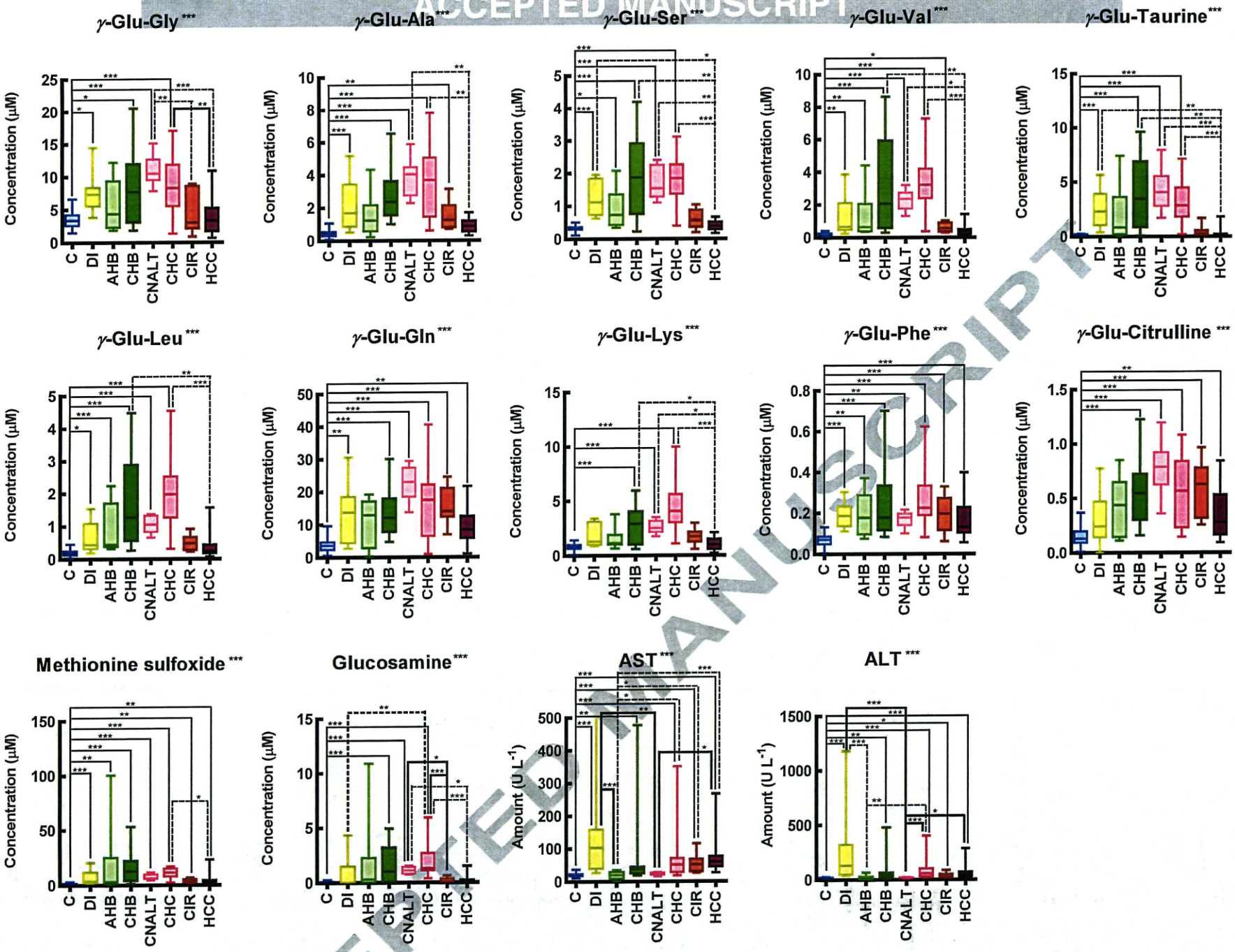

Figure 2 Soga et al.

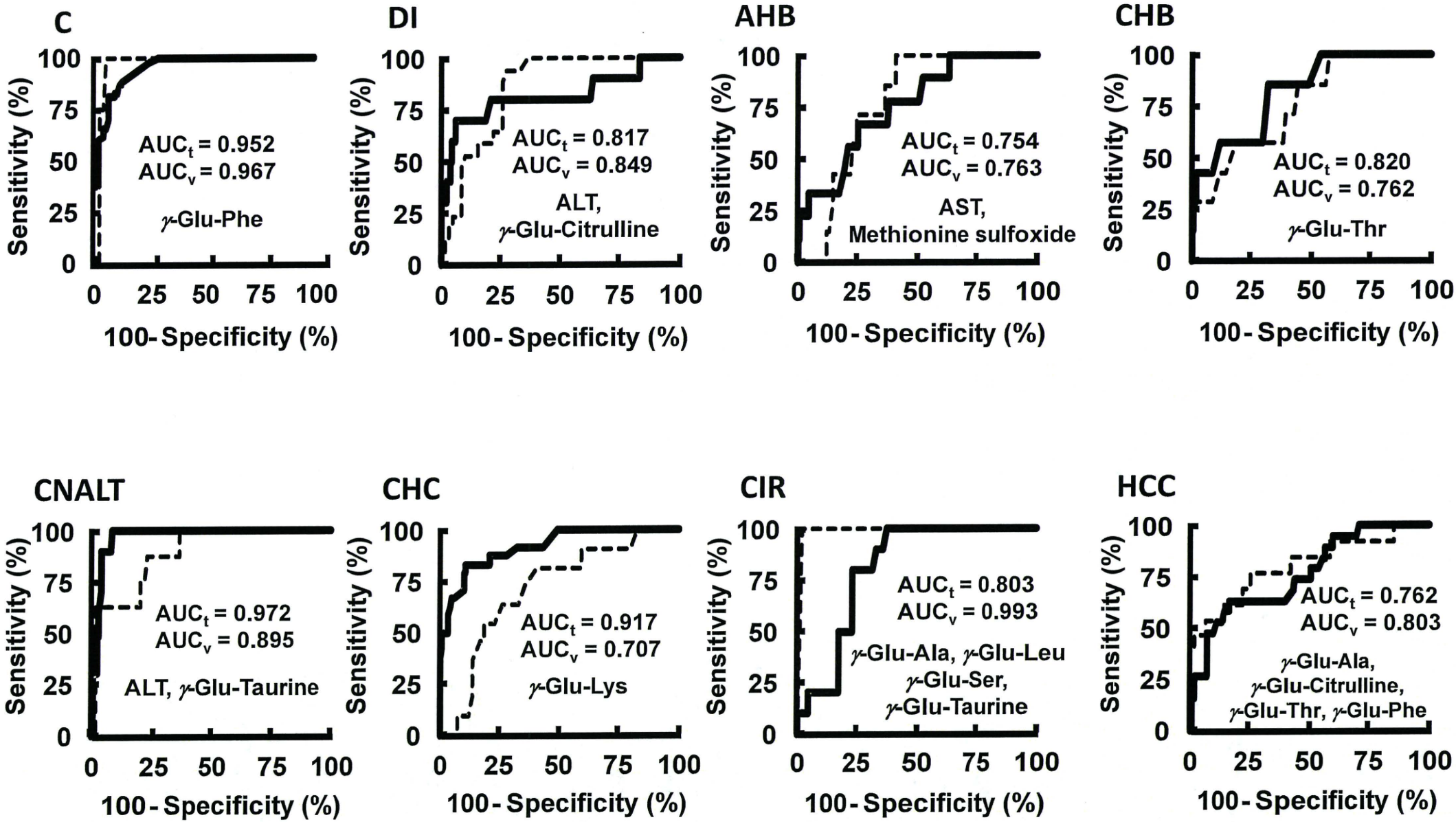

Figure 3 Soga et al.

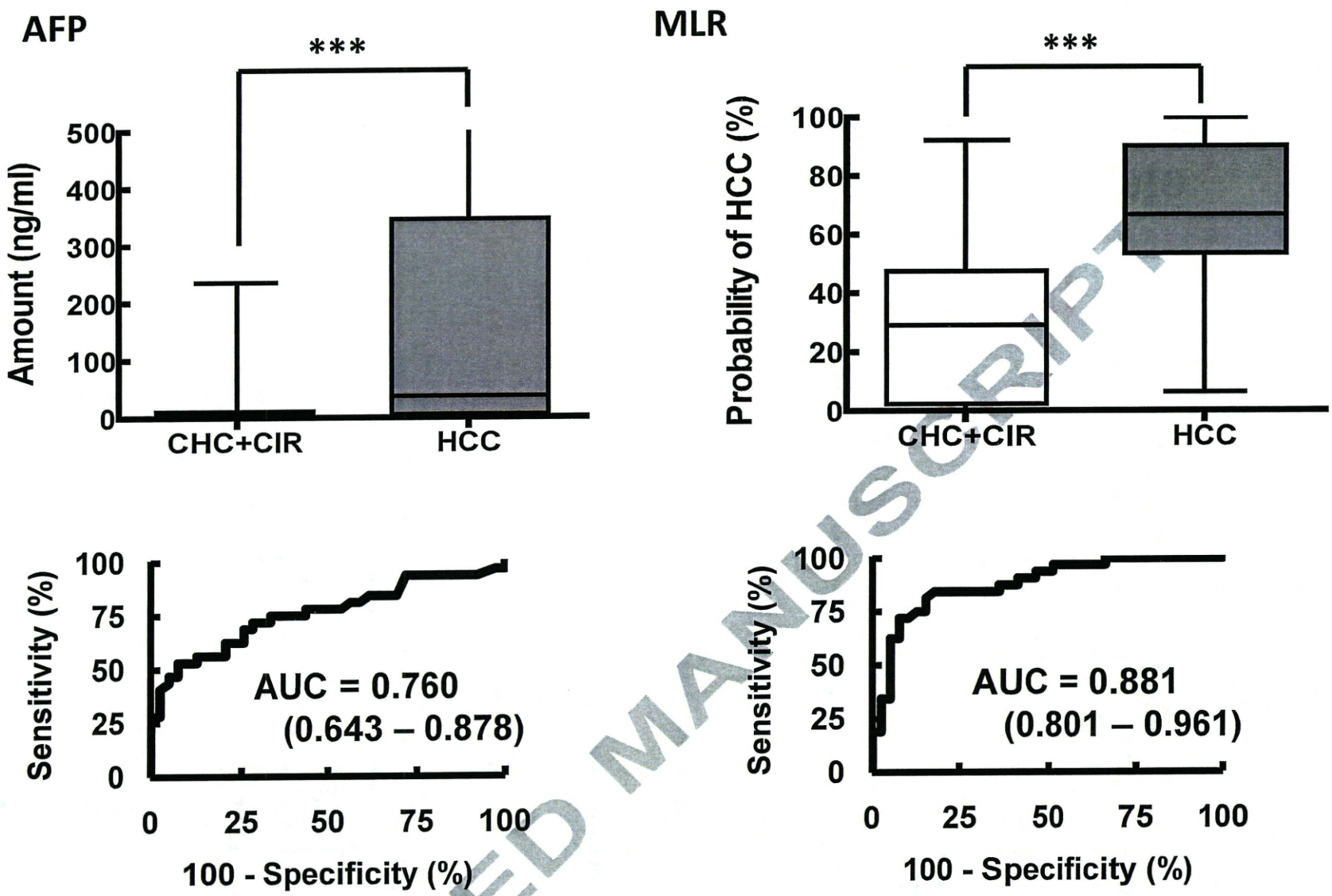

Figure 4 Soga et al.

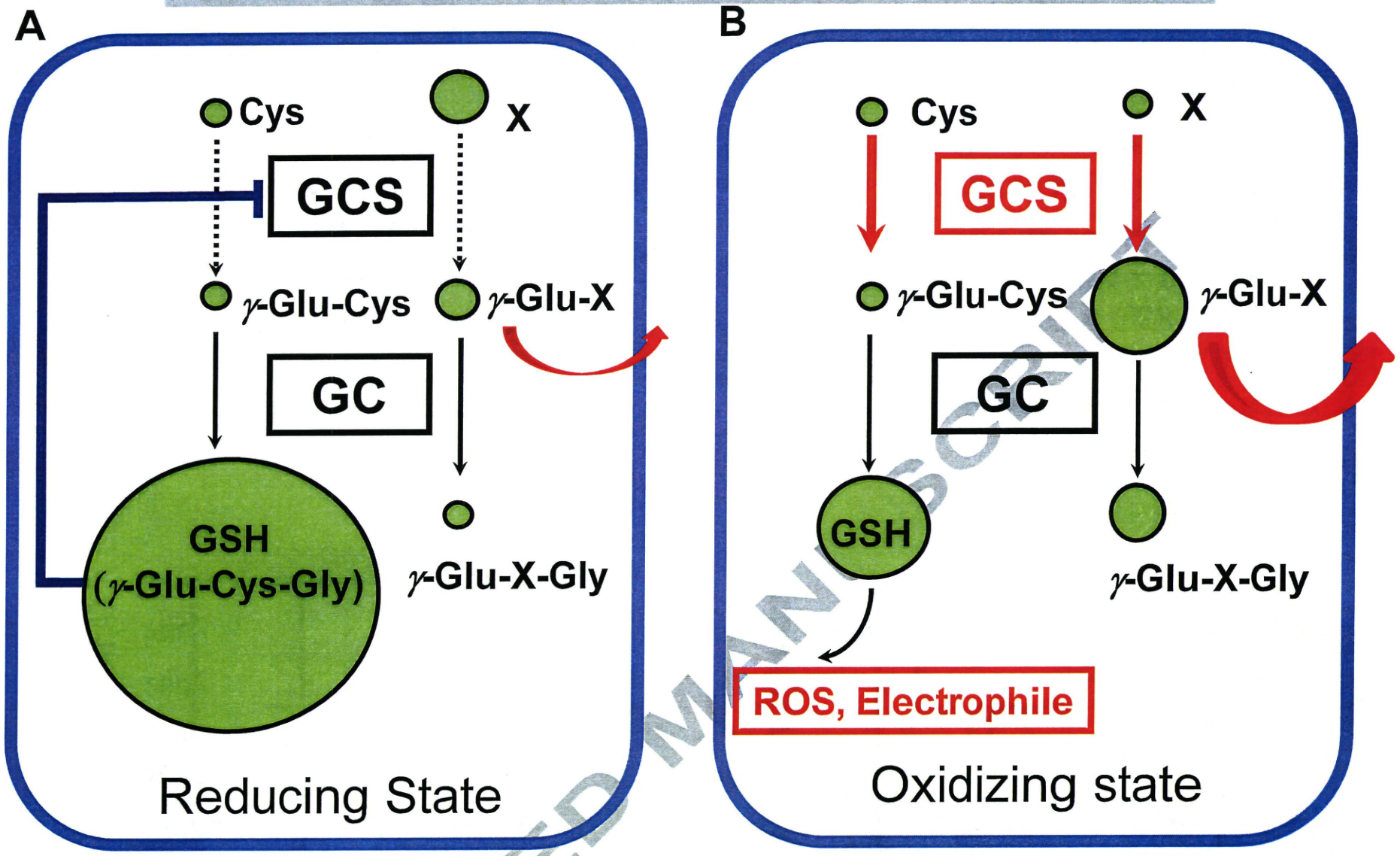

Figure 5 Soga et al.

THE JOURNAL OF BIOLOGICAL CHEMISTRY VOL. 285, NO. 50, pp. 39160–39170, December 10, 2010

Metabolome Analysis Revealed Increase in *S*-Methylcysteine and Phosphatidylisopropanolamine Synthesis upon L-Cysteine Deprivation in the Anaerobic Protozoan Parasite *Entamoeba histolytica*[*] [S]

Received for publication, July 22, 2010, and in revised form, September 23, 2010 Published, JBC Papers in Press, October 5, 2010, DOI 10.1074/jbc.M110.167304

Afzal Husain[‡§1], Dan Sato[¶], Ghulam Jeelani[‡‖2], Fumika Mi-ichi[‡3], Vahab Ali[§4], Makoto Suematsu[‖], Tomoyoshi Soga[¶], and Tomoyoshi Nozaki[‡2,5]

From the [‡]Department of Parasitology, National Institute of Infectious Diseases, 1-23-1 Toyama, Shinjuku-ku, Tokyo 162-8640, Japan, the [§]Department of Parasitology, Gunma University, Graduate School of Medicine, Maebashi 371-8511, Japan, the [¶]Institute for Advanced Biosciences, Keio University, Tsuruoka, Yamagata 997-0052, Japan, and the [‖]Department of Biochemistry and Integrative Medical Biology, School of Medicine, Keio University, Shinjuku, Tokyo 160-8582, Japan

L-Cysteine is ubiquitous in all living organisms and is involved in a variety of functions, including the synthesis of iron-sulfur clusters and glutathione and the regulation of the structure, stability, and catalysis of proteins. In the protozoan parasite *Entamoeba histolytica*, the causative agent of amebiasis, L-cysteine plays an essential role in proliferation, adherence, and defense against oxidative stress; however, the essentiality of this amino acid in the pathways it regulates is not well understood. In the present study, we applied capillary electrophoresis time-of-flight mass spectrometry to quantitate charged metabolites modulated in response to L-cysteine deprivation in *E. histolytica*, which was selected as a model for examining the biological roles of L-cysteine. L-Cysteine deprivation had profound effects on glycolysis, amino acid, and phospholipid metabolism, with sharp decreases in the levels of L-cysteine, L-cystine, and *S*-adenosylmethionine and a dramatic accumulation of *O*-acetylserine and *S*-methylcysteine. We further demonstrated that *S*-methylcysteine is synthesized from methanethiol and *O*-acetylserine by cysteine synthase, which was previously considered to be involved in sulfur-assimilatory L-cysteine biosynthesis. In addition, L-cysteine depletion repressed glycolysis and energy generation, as it reduced acetyl-CoA, ethanol, and the major nucleotide di- and triphosphates, and led to the accumulation of glycolytic intermediates. Interestingly, L-cysteine depletion increased the synthesis of isopropanolamine and phosphatidylisopropanolamine, and it was confirmed that their increment was not a result of oxidative stress but was a specific response to L-cysteine depletion. We also identified a pathway in which isopropanolamine is synthesized from methylglyoxal via aminoacetone. To date, this study represents the first case where L-cysteine deprivation leads to drastic changes in core metabolic pathways, including energy, amino acid, and phospholipid metabolism.

Sulfur-containing amino acids are essential for all living organisms from bacteria to higher eukaryotes and play indispensable roles in various cellular processes, such as methylation and the generation of polyamines, iron-sulfur clusters, and antioxidants. L-Cysteine in particular is essential for the structure, stability, and various protein functions, including catalysis, electron transfer, redox regulation, nitrogen fixation, and sensing for regulatory processes (1).

Entamoeba histolytica is an enteric protozoan parasite that causes hemorrhagic dysentery and extraintestinal abscesses in millions of inhabitants of endemic areas (2). This parasite is generally considered as anaerobic/microaerophilic and has been shown to consume oxygen and tolerate low levels of oxygen pressure but lacks most of the components of antioxidant defense mechanisms, such as catalase, peroxidase, glutathione, and the glutathione-recycling enzymes glutathione peroxidase and glutathione reductase (3, 4). L-Cysteine, which replaces glutathione as a major thiol in *E. histolytica*, is synthesized via a sulfur assimilatory *de novo* cysteine biosynthetic pathway (5–9) that is typically present in bacteria and plants. This pathway consists of two steps that are catalyzed by serine acetyltransferase (SAT, EC 2.3.1.30)[6]

* This work was supported by Grants-in-Aid for Scientific Research 18GS0314, 18050006, and 18073001 (to T. N.) and 20590429 (to D. S.) from the Ministry of Education, Culture, Sports, Science and Technology of Japan, Grant H20-Shinkosaiko-016 for research on emerging and re-emerging infectious diseases from the Ministry of Health, Labour and Welfare of Japan, and a grant for research to promote the development of anti-AIDS pharmaceuticals from the Japan Health Sciences Foundation (to T. N.).

[S] The on-line version of this article (available at http://www.jbc.org) contains supplemental Fig. S1.

[1] Supported by the Monbukagakusho Scholarship from the Ministry of Education, Culture, Sports, Science and Technology.

[2] Supported by the Global Center of Excellence Program for Human Metabolomic System Biology of the Ministry of Education Culture, Sports, Science and Technology.

[3] Present address: Division of Molecular and Cellular Immunoscience, Dept. of Biomolecular Sciences, Saga University, Saga 849-8581, Japan.

[4] Present address: Dept. of Biochemistry, Rajendra Memorial Research Institute of Medical Sciences, Agamkuan, Patna-800007, India.

[5] To whom correspondence should be addressed: Dept. of Parasitology, National Institute of Infectious Diseases, 1-23-1 Toyama, Shinjuku-ku, Tokyo 162-8640, Japan. Tel.: 81-3-5285-1111, Ext. 2600; Fax: 81-3-5285-1219; E-mail: nozaki@nih.go.jp.

[6] The abbreviations used are: SAT, serine acetyltransferase; CS, cysteine synthase; CE-TOFMS, capillary electrophoresis time-of-flight mass spectrometry; 2′,7′-DCF-DA, 2′,7′-dichlorodihydrofluorescein di-acetate; ESI, electrospray ionization; Cho, choline; Cho-P, choline phosphate; OAS, *O*-acetylserine; SMC, *S*-methylcysteine; SAM, *S*-adenosylmethionine; Ispn, isopropanolamine; Ispn-P, isopropanolamine phosphate; PtdIspn, phosphatidylisopropanolamine; Etn, ethanolamine; Etn-P, ethanolamine phosphate; PtdEtn, phosphatidylethanolamine.

(7, 8) and cysteine synthase (CS; OAS (thiol) lyase; EC 4.2.99.8) (5). In addition to the presence of prokaryotic/plant-like L-cysteine biosynthesis, *E. histolytica* is also unique because the forward and reverse trans-sulfuration pathways are absent and interrupted, respectively. Furthermore, through lateral gene transfer from archaea, *E. histolytica* has acquired methionine γ-lyase (EC 4.4.1.11), an enzyme that degrades L-methionine, L-homocysteine, and L-cysteine (10–12). Thus, although typical parasitic protists show degenerated amino acid metabolic pathways, particularly those associated with catabolism, because of the parasitic lifestyle, sulfur-containing amino acid metabolism appears to have uniquely evolved in *E. histolytica*. However, the specific role of this pathway in this organism remains unclear.

L-Cysteine is the principal low molecular weight thiol in *E. histolytica* and is involved in the survival, growth, attachment, elongation, motility, gene regulation, and antioxidative stress defense of this organism (13–17). Because sulfur-containing amino acid metabolism differs significantly between *E. histolytica* and its mammalian host, the molecular dissection and characterization of this pathway may lead to the development of new chemotherapeutics against this parasite (18).

Here, to gain further insight into the roles and regulatory mechanisms of sulfur-containing amino acid metabolism and individual metabolites in *E. histolytica*, we utilized capillary electrophoresis time-of-flight mass spectrometry (CE-TOFMS) (19–21) for the metabolomic profiling of this parasite. We observed drastic changes in the metabolome as a result of L-cysteine depletion, which led to the discovery of novel L-cysteine-mediated regulation of several metabolic pathways in *E. histolytica*.

EXPERIMENTAL PROCEDURES

Chemicals and Reagents—All of the chemicals of analytical grade were purchased from either Wako or Sigma-Aldrich unless otherwise mentioned. 2′,7′-Dichlorodihydrofluorescein di-acetate (2′,7′-DCF-DA) was purchased from Invitrogen. 1-Aminoacetone hydrochloride was obtained from United States Biologicals. High performance thin layer chromatography silica gel 60 plates were purchased from Merck. [U-$^{13}C_5$,^{15}N]L-Methionine and [U-$^{13}C_3$,^{15}N]L-serine were purchased from Cambridge Isotope Laboratories. Stock solutions of metabolite standards (1–100 mmol/liter) for CE-MS analysis were prepared in either Milli-Q water, 0.1 mol/liter HCl, or 0.1 mol/liter NaOH. A mixed solution of the standards was prepared by diluting stock solutions with Milli-Q water immediately before CE-TOFMS analysis.

Microorganisms and Cultivation—Trophozoites of the *E. histolytica* clonal strain HM-1: IMSS cl 6 were maintained axenically in Diamond's BI-S-33 medium at 35.5 °C, as described previously (22, 23). Trophozoites were harvested in the late logarithmic growth phase 2–3 days after the inoculation of medium with one-thirtieth to one-twelfth of the total culture volume.

Metabolic Labeling and Metabolite Extraction—*E. histolytica* trophozoites were cultivated in either standard BI-S-33 medium containing 8 mM L-cysteine or L-cysteine-deprived medium for 48 h. For the metabolic labeling, trophozoites were cultured in the presence of either 3 mM stable isotope-labeled [U-$^{13}C_5$,^{15}N]L-methionine or 6 mM [U-$^{13}C_3$,^{15}N]L-serine in L-cysteine-deprived medium for 48 h as described above. To extract metabolites, ~1.5×10^6 cells from each condition were harvested and washed twice with 5% mannitol. The cells were then suspended in 1.6 ml of methanol containing 16 μM of each internal standard, 2-(*N*-morpholino)ethanesulfonic acid, methionine sulfone, and D-camphor-10-sulfonic acid and mixed with 1.6 ml of chloroform and 640 μl of deionized water. After vortexing, the mixture was centrifuged at 4,600 × *g* at 4 °C for 5 min. The aqueous layer (1.6 ml) was filtrated using an Amicon Ultrafree-MC ultrafilter (Millipore Co.) and centrifuged at 9,100 × *g* at 4 °C for ~2 h. The filtrate was dried and preserved at −80 °C until mass spectrometric analysis (24). Prior to the analysis, the sample was dissolved in 20 μl of deionized water containing reference compounds (200 μmol/liter each of 3-aminopyrrolidine and trimesic acid).

Instrumentation and CE-TOFMS Conditions—CE-TOFMS was performed using an Agilent CE capillary electrophoresis system equipped with an Agilent 6210 time-of-flight mass spectrometer, Agilent 1100 isocratic HPLC pump, Agilent G1603A CE-MS adapter kit, and Agilent G1607A CE-ESI-MS sprayer kit (Agilent Technologies, Waldbronn, Germany). The system was controlled by Agilent G2201AA ChemStation software for CE. Data acquisition was performed by Analyst QS software for Agilent TOF (Applied Biosystems and MDS Sciex).

CE-TOFMS Conditions for Cationic Metabolite Analysis—Cationic metabolites were separated in a fused silica capillary (50-μm inner diameter × 100-cm) filled with 1 mol/liter formic acid as the reference electrolyte (25). Sample solution (~3 nl) was injected at 50 mbar for 3 s, and a positive voltage of 30 kV was applied. The capillary and sample trays were maintained at 20 °C and below 5 °C, respectively. Sheath liquid composed of methanol/water (50% v/v) that contained 0.1 μmol/liter hexakis (2,2-difluorothoxy)phosphazene was delivered at 10 μl/min. ESI-TOFMS was operated in the positive ion mode. The capillary voltage was set at 4 kV, and a flow rate of nitrogen gas (heater temperature, 300 °C) was set at 10 p.s.i. For TOFMS, the fragmenter voltage, skimmer voltage, and octapole radio frequency voltage (Oct RFV) were set at 75, 50, and 125 V, respectively. An automatic recalibration function was performed using two reference masses of reference standards; protonated [^{13}C]methanol dimer (*m/z* 66.063061) and protonated hexakis (2,2-difluorothoxy)phosphazene (*m/z* 622.028963), which provided the lock mass for exact mass measurements. Exact mass data were acquired at the rate of 1.5 cycles/s over a 50–1,000 *m/z* range.

CE-TOFMS Conditions for Anionic Metabolite Analysis—Anionic metabolites were separated in a cationic polymer-coated COSMO(+) capillary (50-μm inner diameter × 110-cm) (Nacalai Tesque) filled with 50 mmol/liter ammonium acetate solution, pH 8.5, as the reference electrolyte (26, 27). Sample solution (~30 nl) was injected at 50 mbar for 30 s, and a negative voltage of −30 kV was applied. Ammonium acetate (5 mmol/liter) in methanol/water (50% v/v) that contained 0.1 μmol/liter hexakis (2,2-difluorothoxy)phosphazene was delivered as sheath liquid at 10 μl/min. ESI-TOFMS was operated

in the negative ion mode. The capillary voltage was set at 3.5 kV. For TOFMS, the fragmenter voltage, skimmer voltage, and Oct RFV were set at 100, 50, and 200 V, respectively (27). An automatic recalibration function was performed using two reference masses of reference standards: deprotonated ^{13}C acetate dimer (m/z 120.038339) and acetate adduct of hexakis (2,2-difluorothoxy)phosphazene (m/z 680.035541). The other conditions were identical to those used for the cationic metabolite analysis.

CE-TOFMS Data Processing—Raw data were processed using the in-house software Masterhands (28). The overall data processing flow consisted of the following steps: noise filtering, baseline removal, migration time correction, peak detection, and integration of peak area from a 0.02 m/z-wide slice of the electropherograms. This process resembled the strategies employed in widely used data processing software for LC-MS and GC-MS data analysis, such as MassHunter (Agilent Technologies) and XCMS (29). Subsequently, accurate m/z values for each peak were calculated by Gaussian curve fitting in the m/z domain, and migration times were normalized using alignment algorithms based on dynamic programming (19, 30). All of the target metabolites were identified by matching their m/z values and normalized migration times with those of standard compounds in the in-house library.

Quantitation of Reactive Oxygen Species—Fluorescence spectrophotometry was used to measure the production of intracellular reactive oxygen species using 2′,7′-DCF-DA as a probe as previously described (31). Briefly, *E. histolytica* cells were washed in PBS, and 5.0×10^5 cells were then incubated in 1 ml of PBS containing 20 μM 2′,7′-DCF-DA for 30 min at 35.5 °C in the dark. The intensity of fluorescence was immediately read at excitation and emission wavelengths of 492 and 519 nm, respectively.

L-Cysteine/SMC Synthase Assay—L-Cysteine/SMC synthase was assayed by measuring acetate production through the coupling reaction of this enzyme with acetate kinase, pyruvate kinase, and lactate dehydrogenase. Acetate kinase generates ADP and acetyl-phosphate from acetate and ATP. The ADP production was coupled with the oxidation of NADH (ϵ_{340} = 6.22 mM^{-1} cm^{-1}) through pyruvate kinase and lactate dehydrogenase (32). The standard reaction mixture contained 50 mM of Tris-Cl, pH 8.0, 3 mM OAS, 3 mM sodium sulfide or sodium methanethiolate, 4 units each of acetate kinase, pyruvate kinase, and lactate dehydrogenase, 0.5 mM ATP, 0.3 mM NADH, and 1–2 μg of recombinant cysteine synthase. The reactions were initiated by the addition of recombinant cysteine synthase, and optical absorbance was read at 340 nm on a Shimadzu spectrophotometer. Kinetic parameters were determined using various concentrations (0.1–6 mM) of sodium sulfide, sodium methanethiolate, and OAS. The kinetic parameters were estimated using the nonlinear regression function obtained from the GraphPad Prism software (GraphPad Software Inc., San Diego, CA).

Choline and Ethanol Quantitation—The amount of choline (Cho) in the metabolite extracts was quantitated enzymatically using components of the Amplex® Red sphingomyelinase assay kit (Invitrogen). Briefly, Cho was first oxidized by Cho oxidase to betaine and hydrogen peroxide. The produced hydrogen peroxide was then reacted with Amplex® Red reagent in a 1:1 stoichiometry in the presence of horseradish peroxidase to generate the highly fluorescent product resorufin, which was read in a fluorescence spectrophotometer (model F-2500; Hitachi) at excitation and emission wavelengths of 545 and 590 nm, respectively. Ethanol production by trophozoites cultured in either normal or L-cysteine-deprived medium was determined as described previously (33).

Extraction of Lipids, Thin Layer Chromatography, and Phospholipid Quantitation—Cells cultured in either normal or cysteine-deprived medium for 48 h were collected by centrifugation, and lipids were then extracted by the Bligh and Dyer's method (34). The extracted lipids were analyzed by two-dimensional high performance thin layer chromatography using a solvent system of chloroform:methanol:28% ammonium hydroxide (65:25:5 v/v/v) in the first direction and chloroform:acetone:methanol:Acetic acid:water (50:20:10:10:5 v/v/v/v/v) in the second. The phosphorus content of phospholipids was determined after scraping representative spots from the plate, as described previously (35). The lipids were visualized by exposing TLC plates to iodine vapor.

RESULTS

L-Cysteine Deprivation Caused Accumulation of O-Acetylserine and S-Methylcysteine—We first verified that L-cysteine deprivation affected intracellular L-cysteine/L-cystine concentrations in *E. histolytica*. Under normal culture conditions (8 mM L-cysteine), the intracellular concentrations of L-cysteine and L-cystine were 431 ± 52 and 202 ± 40 pmol, respectively, per 2×10^5 cells. Approximately two-thirds (68 ± 7%) of L-cysteine/L-cystine was present in a reduced form, whereas the remaining third was present in an oxidized form. Upon L-cysteine deprivation for 48 h, both L-cysteine and L-cystine decreased to nearly undetectable levels (88 ± 11 and 79 ± 10% decrement, respectively) (Fig. 1*A*). These results suggest that the intracellular L-cysteine/L-cystine concentrations in *E. histolytica* are greatly affected by the composition of the extracellular milieu.

We also examined whether oxidative stress induced by paraquat affected intracellular L-cysteine/L-cystine concentrations. Treatment of the amebae with 2 mM paraquat for 10 h led to 60.6 ± 8.8 and 41.4 ± 7.3% decreases in the levels of L-cysteine and L-cystine, respectively. Under conditions of L-cysteine limitation, the intracellular levels of reactive oxygen species increased by >4-fold, which was comparable with the 3.3-fold increase observed in paraquat/air-treated cells (Fig. 1*B*). These results suggest that L-cysteine may be an important scavenger of reactive oxygen species in *E. histolytica*.

Among the ~90 intermediary metabolites that were measured by CE-TOFMS-based metabolomic analysis, which include amino acids, organic acids, and nucleotides (19–21), L-cysteine depletion caused drastic changes in the metabolites of *E. histolytica* involved in sulfur-containing amino acid metabolism (Fig. 1*C*). L-Cysteine depletion resulted in a sharp increase in *O*-acetylserine (OAS) (nearly undetectable under normal conditions), an activated form of L-serine that is synthesized from L-serine and acetyl-CoA by SAT. We also ob-

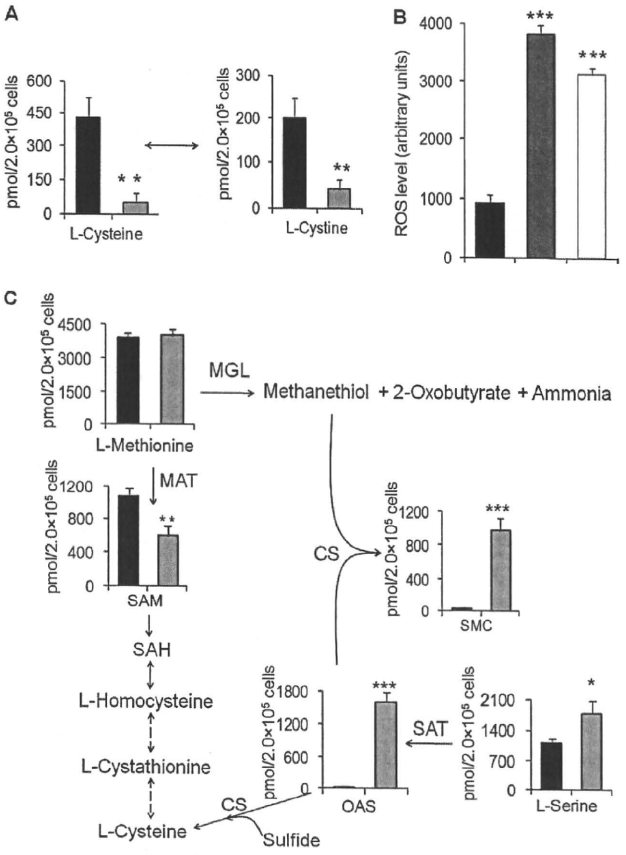

FIGURE 1. **Effects of L-cysteine depletion on the content of L-cysteine/L-cystine, reactive oxygen species, and metabolites in sulfur-containing amino acid metabolism in *E. histolytica*.** Trophozoites were cultured in normal (*black bars*) or cysteine-deprived medium (*gray bars*) for 48 h, or normal medium containing 2 mM paraquat (*white bars*) for 10 h. *Asterisks* (*, **, and ***) denote statistically significant differences with $p \leq 0.05$, $p \leq 0.01$, and $p \leq 0.001$, respectively, as determined by Student's *t* test, and all of the experiments were performed in triplicate. *A*, effects of L-cysteine depletion on intracellular L-cysteine and L-cystine concentrations. The average content (pmol) ± S.D (*error bars*) in 2×10^5 cells is shown. *B*, effects of L-cysteine depletion (72 h) and oxidative stress on the level of reactive oxygen species. The average level of 2′,7′-DCF-DA fluorescence (arbitrary units) ± S.D. (*error bars*) of 5×10^5 cells is shown. *C*, effects of L-cysteine depletion on the level of metabolites involved in sulfur-containing amino acid metabolism. The average content (pmol) ± S.D. (*error bars*) in 2×10^5 cells, performed in triplicate, is shown. *SAH*, *S*-adenosylhomocysteine; *MAT*, L-methionine adenosyltransferase; *MGL*, L-methionine γ-lyase.

served a marked increase (nearly undetectable under normal conditions) in *S*-methylcysteine (SMC), which is suggested to be a storage compound for sulfide and methyl groups in plants (36). L-Cysteine deprivation also caused a 44 ± 6% decrement in the level of *S*-adenosylmethionine (SAM), whereas the level of L-methionine remained unchanged.

SMC can be formed by the methylation of L-cysteine using either SAM or *S*-methylmethionine as a methyl group donor or by the transfer of the alanyl moiety of OAS to methanethiol (CH_3SH) by CS (37). To differentiate between these possibilities, we performed metabolic labeling of *E. histolytica* trophozoites with stable isotope U-^{13}C,^{15}N-labeled L-serine and L-methionine in normal and L-cysteine-depleted media for 48 h. Upon the addition of [U-$^{13}C_3$,^{15}N]Ser to the L-cysteine-depleted culture medium, comparable levels of [$^{13}C_3$,^{15}N]SMC and unlabeled SMC, derived from [U-$^{13}C_3$,^{15}N]OAS and unlabeled OAS, respectively, were detected (Fig. 2*A*). Similarly, when trophozoites were cultured in the presence of [U-$^{13}C_5$,^{15}N]Met under the L-cysteine-deprived conditions, we also detected comparable levels of [$^{13}C_1$]SMC and unlabeled SMC (Fig. 2*B*). In contrast, under normal conditions, neither SMC nor OAS was detected after [U-$^{13}C_3$,^{15}N]Ser or [U-$^{13}C_5$,^{15}N]Met labeling (data not shown). Taken together, these data clearly indicate that SMC is not synthesized by SAM- or *S*-methylmethionine-dependent methylation of L-cysteine; rather, SMC is synthesized in *E. histolytica* from the backbone of Ser and thiomethyl group of methanethiol.

Surprisingly, [$^{13}C_3$,^{15}N]OAS was not incorporated into either L-cysteine or L-cystine (data not shown), or their levels were too low to be detected by CE-TOFMS. To determine whether the lack of OAS incorporation into L-cysteine was due to the low sulfide concentrations under the *in vitro* axenic growth conditions, we deprived trophozoites of L-cysteine for 45 h and then continued their culture in medium supplemented with 2 mM sulfide for a further 3 h. However, sulfide supplementation did not affect the level of L-cysteine, whereas the levels of SMC and OAS markedly decreased (90.6 ± 3.4 and 84.8 ± 7.7% decrement, respectively) compared with the unsupplemented medium (Fig. 2*C*). These data suggest that sulfide negatively regulates OAS and SMC synthesis and also imply that the pathway formally called the "L-cysteine biosynthetic pathway" is primarily involved in the synthesis of SMC, but not L-cysteine, at least under *in vitro* culture conditions.

In Vitro Examination of S-Methylcysteine Synthesis—To elucidate the enzyme(s) involved in the formation of SMC from OAS and methanethiol, we examined whether different CS isotypes could catalyze the synthesis of SMC. Among the three examined CS isotypes (EhCS1–3), two CS proteins (EhCS1 and EhCS2) are very similar (99% amino acid identity, with two conserved amino acid changes) (5, 6), whereas EhCS3 shares only 83% amino acid identity with the other two isotypes. Both recombinant EhCS1 and EhCS3 efficiently catalyzed the synthesis of SMC using OAS and methanethiol as substrates. As revealed from the kinetic parameters (Fig. 2*D*), EhCS1 and EhCS3 did not show any preference for either methanethiol or sulfide, because the K_m, V_{max}, k_{cat}, and k_{cat}/K_m values for both of these substrates were comparable.

L-Cysteine Depletion Repressed Glycolysis and Energy Generation—Similar to other anaerobic and microaerophilic parasitic protozoa, such as *Giardia lamblia* and *Trichomonas vaginalis*, *E. histolytica* lacks features of aerobic eukaryotic metabolism, including the TCA cycle and oxidative phosphorylation, and primarily generates energy by substrate level phosphorylation (10). The CE-TOFMS-based metabolomic analysis demonstrated that L-cysteine depletion affected the levels of the majority of metabolites involved in glycolysis and its associated pathways (Fig. 3). L-Cysteine-depleted amebae generally contained higher amounts of glycolytic intermediates, with the exception of acetyl CoA and ethanol, than cells cultured under normal conditions. The largest changes caused by L-cysteine depletion were the increment in the levels of glycerol-3-phosphate (2.18 ± 0.25-fold), *O*-phosphoserine (1.70 ± 0.22-fold), pyruvate (1.66 ± 0.26-fold), 3-phosphoglycerate (1.60 ± 0.17-fold), malate (1.50 ± 0.20-fold),

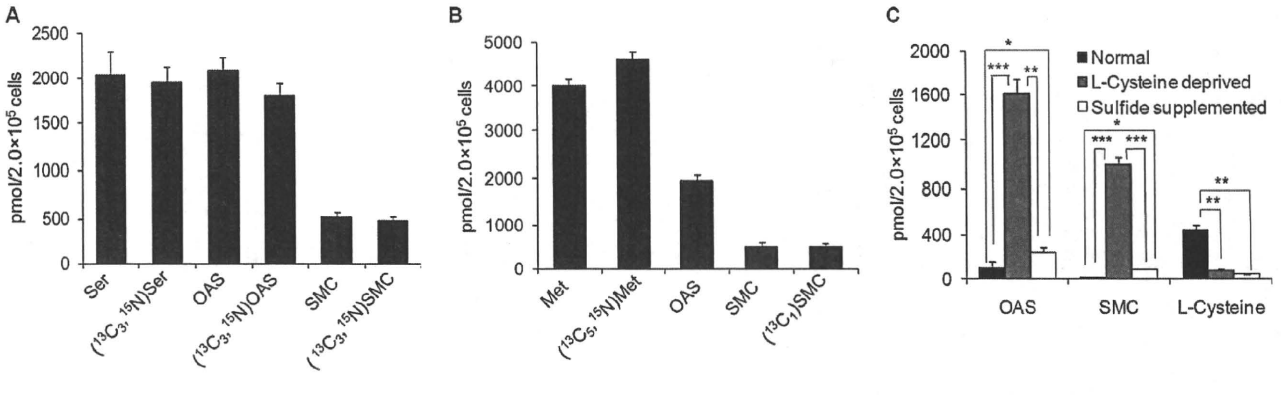

D

	EhCS1				EhCS3			
	Km (mM)	*Vmax* (μmol/min/mg)	*kcat* (s^{-1})	*Kcat/Km* ($mM^{-1}s^{-1}$)	*Km* (mM)	*Vmax* (μmol/min/mg)	*kcat* (s^{-1})	*Kcat/Km* ($mM^{-1}s^{-1}$)
OAS	2.34±0.32	36.20±5.43	22.07±3.26	9.43±2.12	2.54±0.28	31.96±.4.68	19.37±2.98	7.61±2.09
Sulfide	2.01±0.40	35.59±6.21	21.71±3.98	10.81±2.33	2.23±0.34	31.42±5.79	19.08±3.56	8.56±2.24
Methanethiolate	1.66±0.39	25.51±4.78	15.57±2.84	9.37±3.08	2.11±0.39	21.74±3.94	11.22±2.37	5.32±1.88

FIGURE 2. **Examination of *S*-methylcysteine biosynthesis in *E. histolytica*.** *A* and *B*, incorporation of labeled L-serine and L-methionine into *S*-methylcysteine. Trophozoites were cultured in the presence of 6 mM [U-$^{13}C_3$,^{15}N]L-serine (*A*) or 3 mM [U-$^{13}C_5$,^{15}N]L-methionine (*B*) in L-cysteine-deprived medium for 48 h. The average contents (pmol) ± S.D. (*error bars*) of unlabeled and labeled amino acids and their derivatives in 2×10^5 trophozoites, performed in triplicate, are shown. *C*, effects of the supplementation of the medium with sodium sulfide (2 mM) on the levels of OAS, SMC, and L-cysteine, under conditions of L-cysteine deprivation. *Asterisks* (*, **, and ***) denote statistically significant differences with $p \leq 0.05$, $p \leq 0.01$, and $p \leq 0.001$, respectively, as determined by Student's *t* test. *D*, kinetic parameters of recombinant cysteine synthase 1 (EhCS1) and 3 (EhCS3). All of the reactions were performed in triplicate as described under "Experimental Procedures," and the values are expressed as the means ± S.D.

and fumarate (1.60 ± 0.20-fold). Several other metabolites involved in glycolysis, including glucose 6-phosphate, glucose 1-phosphate, fructose 6-phosphate, and phosphoenolpyruvate also showed slightly elevated levels (1.2–1.5-fold), whereas the levels of fructose 1,6-bisphosphate and dihydroxyacetonephosphate remained unchanged. In contrast to the significant increases in the glycolytic intermediates upstream of pyruvate in amebae cultured under L-cysteine-limited conditions, we observed reduced levels of acetyl CoA (29.4 ± 7.1%) and ethanol (40.7 ± 6.7%), suggesting a decrease in glycolytic flux and ATP generation by L-cysteine depletion. A number of other metabolites downstream of acetyl CoA, such as *N*-acetyl-glutamate, *N*-acetyl β-alanine, *N*-acetyl-leucine, and *N*-acetyl-phenylalanine, were also decreased (supplemental Fig. S1), supporting the premise that the glycolytic flux downstream of pyruvate was repressed.

Because glycolysis is the major source of energy generation in *E. histolytica*, a reduced glycolytic flux was thought to result in a decrement in the energy storage molecules of the trophozoites. As expected, the levels of the nucleotide triphosphates ATP, GTP, UTP, and CTP were significantly lower ($p \leq 0.05$) in the L-cysteine-depleted cells than in the trophozoites maintained under normal conditions (Fig. 3). We also observed slight deceases in the levels of ADP and GDP, whereas the levels of AMP and GMP were unchanged (Fig. 3).

L-Cysteine Depletion Altered Amino Acid Pools—Because amino acids are also used for energy production in *E. histolytica* (38), we examined the effects of L-cysteine deprivation on amino acid levels (supplemental Fig. S1). Next to L-cysteine and L-cystine, L-threonine and L-serine were the most highly modulated by L-cysteine depletion (1.63 ± 0.25- and 2.07 ± 0.29-fold increases, respectively) among the 20 amino acids. In *E. histolytica*, L-threonine and L-serine are catabolized by threonine dehydratase (39) to yield 2-oxobutyrate and pyruvate, respectively, which are in turn used by pyruvate:ferredoxin oxidoreductase for energy generation (40). L-Cysteine depletion also resulted in a slight increase in the intracellular concentration of L-alanine, which is synthesized from pyruvate by L-alanine:2-oxoglutarate aminotransferase (EHI_096750 (EAL50292.1) and EHI_159710 (EAL44861.1)). The levels of the remaining amino acids were not significantly affected by L-cysteine depletion.

L-Cysteine Depletion Caused Increases in Isopropanolamine, Aminoalcohol Phosphates, and Phosphatidylisopropanolamine—The metabolomic analysis of *E. histolytica* also revealed that L-cysteine depletion caused marked changes in amino alcohol metabolism (Fig. 4*A*). L-Cysteine depletion led to a dramatic increase in the levels of isopropanolamine (1-aminopropan-2-ol, Ispn) (5.44 ± 0.76-fold) and isopropanolamine phosphate (Ispn-P, undetected under normal conditions) (Fig. 4*A*). In addition, trophozoites cultured in L-cysteine-limited conditions showed 7.01 ± 1.38- and 2.8 ± 0.21-fold increases in ethanolamine phosphate (Etn-P) and choline phosphate (Cho-P) levels, respectively, whereas the levels of ethanolamine (Etn) and Cho were unchanged. Both Etn-P and Cho-P are intermediates in the Kennedy pathway,

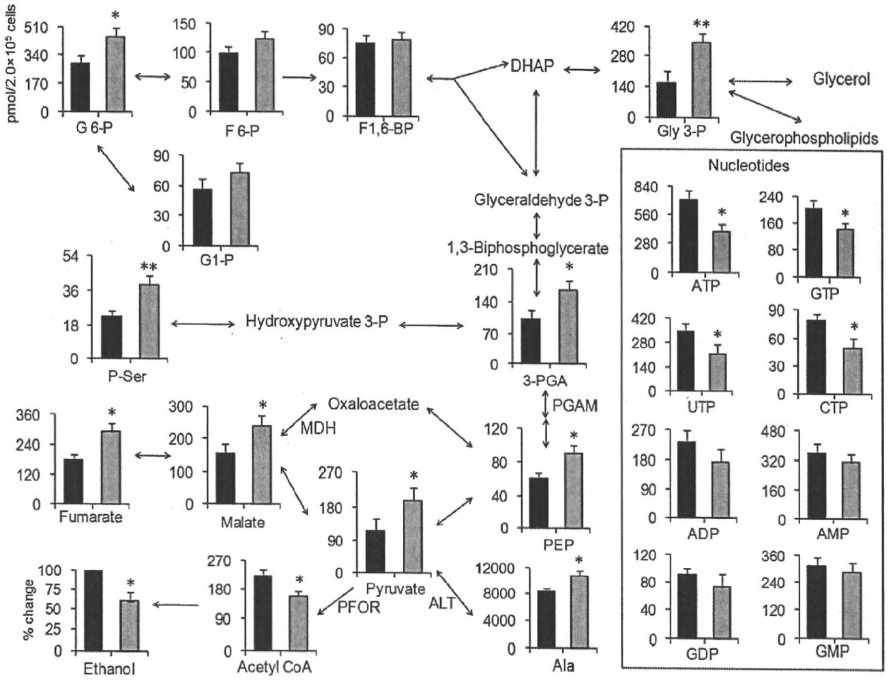

FIGURE 3. **Effects of L-cysteine depletion on the level of metabolites involved in central energy metabolism.** Trophozoites were cultured in normal (*black bars*) or cysteine-deprived medium for 48 h (*gray bars*), and the average contents (pmol) ± S.D. (*error bars*) of the indicated metabolites in 2×10^5 cells are shown (performed in triplicate). Nucleotide metabolites are *boxed*. Ethanol is shown as a percentage change. *Asterisks* (* and **) denote statistically significant differences with $p \leq 0.05$ and $p \leq 0.01$, respectively, as determined by Student's *t* test. *PFOR*, pyruvate:ferredoxin oxidoreductase; *ALT*, L-alanine: 2-oxoglutarate aminotransferase; *PGAM*, phosphoglycerate mutase; *MDH*, malate dehydrogenase; *G 6-P*, glucose 6-phosphate; *G1-P*, glucose 1-phosphate; *F 6-P*, fructose 6-phosphate; *F1,6-BP*, fructose 1,6-biphosphate; *Gly 3-P*, glycerol 3-phosphate; *3-PGA*, 3-phosphoglycerate; *PEP*, phosphoenolpyruvate; *P-Ser*, *O*-phosphoserine.

where phospholipids, including phosphatidylethanolamine and phosphatidylcholine, are produced.

Because L-cysteine limitation affected Ispn-P, Etn-P, and Cho-P concentrations, we next investigated whether L-cysteine deprivation influenced phospholipid synthesis by performing lipid profiling of amebic trophozoites cultured under L-cysteine-deprived or normal conditions using two-dimensional TLC (Fig. 4*B*). We found that in the absence of L-cysteine, *E. histolytica* synthesized an unconventional phospholipid that was verified to be phosphatidylisopropanolamine (PtdIspn) and was undetectable under normal conditions. Quantitation of individual lipids indicated that phosphatidylethanolamine (PtdEtn) decreased by 39.9 ± 6.9%, whereas other phospholipids, such as phosphatidylcholine (PtdCho), phosphatidylserine, phosphatidylinositol, and phosphatidic acid, were unchanged (Fig. 4*C*). These data are consistent with the premise that PtdIspn was formed in a competition for the formation of PtdEtn, the level of which decreased by approximately the identical amount that PtdIspn increased (Fig. 4*C*). To further demonstrate that PtdIspn was formed from Ispn, *E. histolytica* trophozoites were cultured in normal medium containing 5 mM Ispn for 24 h. Under this condition, trophozoites produced an appreciable amount of PtdIspn (Fig. 4*B*, *panel c*).

As described above, L-cysteine depletion increased the level of reactive oxygen species. We therefore examined whether oxidative stress caused the observed changes in amino alcohols and phospholipids. It was observed that the lipid profiling of *E. histolytica* trophozoites cultured with 2 mM paraquat in ambient air for 10 h did not increase PtdIspn (Fig. 4*B*, *panel e*). Furthermore, the addition of D-cysteine to the L-cysteine-lacking medium did not reverse the effects of L-cysteine deprivation on the phospholipid profiles (Fig. 4*B*, *panel d*). These results confirmed that the generation of PtdIspn caused by L-cysteine depletion was not a result of oxidative stress but represents a specific response to L-cysteine deprivation.

Examination of Isopropanolamine Biosynthesis in E. histolytica—Next, we investigated the synthesis route of Ispn in *E. histolytica*. From studies of *Escherichia coli*, it is known that Ispn is synthesized from 1-aminoacetone by the action of Ispn:NAD^+ oxidoreductase (41). 1-Aminoacetone is formed by the breakdown of L-threonine by L-threonine dehydrogenase (42) or is alternatively synthesized from methylglyoxal by monoamine oxidase, which catalyzes the interconversion of methylglyoxal and aminoacetone (43). Methylglyoxal is a by-product of several metabolic pathways, with glycolysis being the most important source (44). Methylglyoxal is synthesized either enzymatically or nonenzymatically from dihydroxyacetone phosphate or glyceraldehyde 3-phosphate (44).

To examine the Ispn synthesis pathway in *E. histolytica*, we cultured amebae in medium supplemented with either methylglyoxal, aminoacetone, or L-threonine and examined the resulting lipid profiles. We found that supplementation with 2 mM methylglyoxal or 4 mM aminoacetone, but not 50 mM L-threonine, led to the synthesis of PtdIspn (Fig. 5*A*). These results are consistent with the premise that *E. histolytica* is capable of Ispn synthesis from methylglyoxal and possesses the

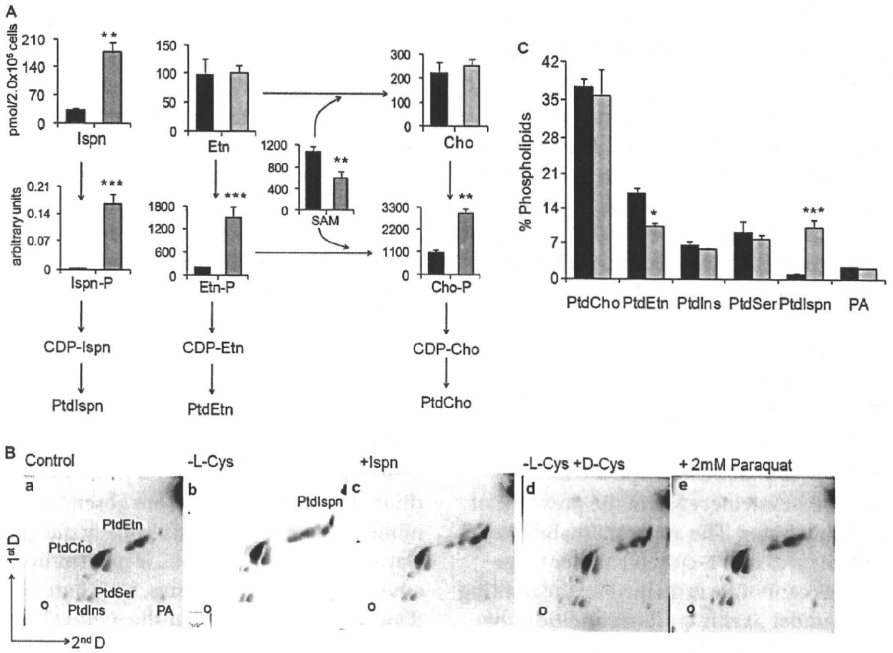

FIGURE 4. **L-Cysteine depletion affected phospholipid metabolism.** *A*, effects of L-cysteine depletion on the levels of metabolites involved in the Kennedy pathway of phospholipid metabolism. Trophozoites were cultured in normal (*black bars*) or cysteine-deprived medium for 48 h (*gray bars*). The average contents (pmol) ± S.D. (*error bars*) in 2×10^5 cells in triplicate are shown. *Asterisks* (*, **, and ***) denote statistically significant differences with $p \leq 0.05$, $p \leq 0.01$, and $p \leq 0.001$, respectively, as determined by Student's *t* test. *B*, profiles of phospholipids derived from trophozoites cultured under various conditions (*panels a–e*), analyzed by two-dimensional TLC. Trophozoites were cultured in normal culture medium (*panels a*, *c*, and *e*) or L-cysteine-deprived medium supplemented (*panels b* and *d*), without (*panels a* and *b*) or with 5 mM Ispn (*panels c*), or 8 mM D-cysteine (*panels d*) for 48 h or 2 mM paraquat for 10 h (*panels e*). *Circles* in the *bottom left corners* indicate the spots where the samples were applied. *C*, quantitation of the phospholipid species (percentage) derived from trophozoites cultured using normal (*black bars*) or L-cysteine-depleted (*gray bars*) medium. *Asterisks* (* and ***) denote statistically significant differences with $p \leq 0.05$ and $p \leq 0.001$, respectively, as determined by Student's *t* test. *PtdSer*, phosphatidylserine; *PtdIns*, phosphatidylinositol; *PA*, phosphatidic acid.

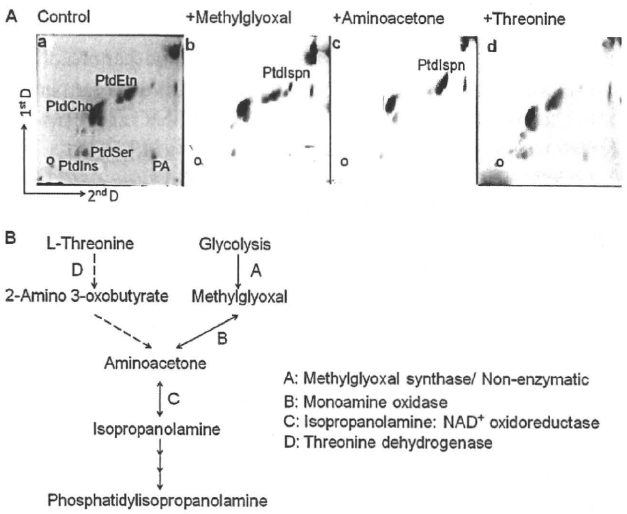

FIGURE 5. **Examination of isopropanolamine biosynthesis in *E. histolytica*.** *A*, effects of the supplementation of potential precursors to the culture medium on the synthesis of phosphatidylisopropanolamine. Trophozoites were cultured in normal culture medium supplemented without (*panel a*) or with 2 mM methylglyoxal (*panel b*), 5 mM aminoacetone (*panel c*), or 50 mM L-threonine for 24 h (*panel d*), and the lipids were then analyzed by two-dimensional TLC. *Circles* in the *bottom left corners* indicate the spots where the samples were applied. *B*, possible pathways of isopropanolamine biosynthesis. The reactions depicted by *solid arrows* were demonstrated in this study, whereas those indicated by *broken arrows* are considered to be absent in *E. histolytica*. *PtdSer*, phosphatidylserine; *PtdIns*, phosphatidylinositol; *PA*, phosphatidic acid.

enzymatic activities of monoamine oxidase and Ispn:NAD^+ oxidoreductase (Fig. 5*B*).

DISCUSSION

Identification of SMC and OAS as the Major Metabolites Increased upon L-Cysteine Deprivation—In the present study, using a CE-TOFMS-based approach (19–21), we identified novel metabolic changes caused by L-cysteine deprivation in the anaerobic/microaerophilic protozoan parasite *E. histolytica*. The major advantages of CE-MS analysis include its extremely high resolution and ability to simultaneously quantify charged low molecular weight compounds (19–21). We demonstrated that L-cysteine deprivation causes a dramatic accumulation of SMC and OAS (Fig. 1*C*). SMC is a sulfur-containing amino acid that has never been detected in protozoa but is widely present in relatively large amounts in several legumes, where it is considered to serve as a sulfur storage compound (36, 37). Using stable isotope-labeled L-serine and L-methionine, we showed that SMC is synthesized from these amino acids in *E. histolytica* via OAS and methanethiol, respectively, which is similar to the pathway reported in *A. thaliana* (36). Interestingly, the increase in both SMC and OAS was mitigated by supplementation of the culture medium with 2 mM sulfide. These results have solved one enigma concerning the biological roles of the sulfur assimilatory *de novo* L-cysteine biosynthetic pathway in *E. histolytica*.

Role of L-Cysteine Biosynthetic Pathway—Although *E. histolytica* is a unique organism that constitutively expresses high